https://doi.org/10.5194/bg-2019-310
Preprint. Discussion started: 13 November 2019

Biogeosciences Discussions
Open Access
EGU

Temporary and net sinks of atmospheric CO_2 due to chemical weathering in subtropical catchment with mixing carbonate and silicate lithology

Yingjie Cao[a,c,d], Yingxue Xuan[b], Changyuan Tang[a,b,c]*, Shuai Guan[e], Yisheng Peng[a,c]

[a]School of Environmental Science and Engineering, Sun Yat-Sen University, Guangzhou, China

[b]School of Geography and Planning, Sun Yat-Sen University, Guangzhou, China

[c]Guangdong Provincial Key Laboratory of Environmental Pollution Control and Remediation Technology, Sun Yat-Sen University, Guangzhou, China

[d]Southern Marine Science and Engineering Guangdong Laboratory, Zhuhai, China

[e]Guangdong Research Institute of Water Resource and Hydropower, Guangzhou, China

Abstract: The study provides the major ion chemistry, chemical weathering rates and temporary and net CO_2 sinks in the Beijiang River, which was characterized as hyperactive region with high chemical weathering rates, carbonate and silicate mixing lithology and abundant sulfuric acid chemical weathering agent with acid deposition and acid mining drainage (AMD) origins. The total chemical weathering rate of 85.46 $t \cdot km^{-2} \cdot a^{-1}$ was comparable to other rivers in the hyperactive zones between the latitude 0-30°. Carbonate weathering rates of 61.15 $t \cdot km^{-2} \cdot a^{-1}$ contributed to about 70% of the total. The lithology, runoff and geomorphology had significant influence on the chemical weathering rate. The proportion of carbonate outcrops had significant positive correlation with the chemical weathering rate. Due to the interaction between dilution and compensation effect, significant positive linear relationship was detected between runoff and total, carbonate and silicate weathering rates. The geomorphology factors such as catchment area, average slope and hypsometric integral value (HI) had non-linear correlation on chemical weathering rate and showed

https://doi.org/10.5194/bg-2019-310
Preprint. Discussion started: 13 November 2019

significant scale effect, which revealed the complexity in chemical weathering processes. DIC-apportionment showed that CCW (Carbonate weathering by CO_2) was the dominant origin of DIC (35%-87%) and that SCW (Carbonate weathering by H_2SO_4) (3%-15%) and CSW (Silicate weathering by CO_2) (7%-59%) were non-negligible processes. The temporary CO_2 sink was 823.41 10^3 mol km^{-2} a^{-1}. Compared with the "temporary" sink, the net sink of CO_2 for the Beijiang River was approximately 23.18×10^3 mol km^{-2} a^{-1} of CO_2 and was about 2.82% of the "temporary" CO_2 sink. Human activities (sulfur acid deposition and AMD) dramatically decreased the CO_2 net sink and even make chemical weathering a CO_2 source to the atmosphere.

Keywords: Chemical weathering, DIC-apportionment, CO_2 temporary sink, CO_2 net sink

1 Introduction

About half of the global CO_2 sequestration due to chemical weathering occurs in warm and high runoff regions (Ludwig et al., 1998), so called the hyperactive regions and hotspots (Meybeck et al., 2006). Chemical weathering driven by weak carbonic acid (H_2CO_3) that originates from atmosphere CO_2 or soil respiration under natural conditions is a fundamental geochemical process regulating the atmosphere-land-ocean fluxes and earth's climate (Guo et al., 2015). Carbonate and silicate weathering define the two typical categories of chemical weathering. A profound case in point is that from the view of the global carbon cycle, the CO_2 consumption due to carbonate weathering is recognized the "temporary" sink because that the flux of CO_2 consumed by carbonate dissolution on the continents is balanced by the flux of CO_2 released into the atmosphere from the oceans by carbonate precipitation on the geological time scale (Cao et al., 2015; Garrels, 1983). While the consumption of CO_2 during the chemical weathering of silicate rocks has been regard as

https://doi.org/10.5194/bg-2019-310
Preprint. Discussion started: 13 November 2019

the net sink of CO_2 and regulates the global carbon cycle (Hartmann et al., 2009; Hartmann et al., 2014b; Kempe and Degens, 1985; Lenton and Britton, 2006). Thus in carbonate-silicate mixing catchment, it is essential to distinguish proportions of the two most important lithological groups, i.e., carbonates and silicates, and evaluate the net CO_2 sink due to chemical weathering of silicate (Hartmann et al., 2009).

In addition to the chemical weathering induced by H_2CO_3, sulfuric acid (H_2SO_4) of anthropogenic origins produced by sulfide oxidation such as acid deposition caused by fossil fuel burning and acid mining discharge (AMD) also becomes an important chemical weathering agent in the catchment scale. Many studies have shown the importance of sulfide oxidation and subsequent dissolution of other minerals by the resulting sulfuric acid at catchment scale (Hercod et al., 1998; Spence and Telmer, 2005). Because depending on the fate of sulfate in the oceans, sulfide oxidation coupled with carbonate dissolution could facilitate a release of CO_2 to the atmosphere (Spence and Telmer, 2005), the carbonate weathering by H_2SO_4 (sulfide oxidation) plays a very important role in quantifying and validating the ultimate CO_2 consumption rate. Thus, under the influence of human activities, the combination of silicate weathering by H_2CO_3 and carbonate weathering by H_2SO_4 controlled the net sink of atmospheric CO_2.

Numerous studies on chemical weathering of larger rivers have been carried out to examine hydrochemical characteristics, chemical erosion and CO_2 consumption rates, and long-term climatic evolution of the Earth in various large rivers, such as the Changjiang River (Chen et al., 2002a; Ran et al., 2010), the Huanghe River (Zhang et al., 1995), the Pearl River (Gao et al., 2009; Xu and Liu, 2010; Zhang et al., 2007a), the Huai River (Zhang et al., 2011), the rivers of the Qinghai-Tibet Plateau (Jiang et al., 2018; Li et al., 2011; Wu et al., 2008), the Mekong River (Li et al., 2014), the

https://doi.org/10.5194/bg-2019-310
Preprint. Discussion started: 13 November 2019

rivers of the Alpine region (Donnini et al., 2016), the Sorocaba River (Fernandes et al., 2016), the rivers of Baltic Sea catchment (Sun et al., 2017), the Amazon River (Gibbs, 1972; Mortatti and Probst, 2003; Stallard and Edmond, 1981; Stallard and Edmond, 1983; Stallard and Edmond, 1987), the Lena River (Huh and Edmond, 1999) and the Orinoco River (Mora et al., 2010). For simplicity of calculation procedure, most of the researches have ignore the sulfuric acid induced chemical weathering and resulted in an overestimation of CO_2 sink. To overcome this shortcoming of traditional mass-balance method, we applied a DIC source apportionment procedure to discriminate the contribution of sulfuric acid induced chemical weathering to validate the temporary and net sink of CO_2 in a typical hyperactive region with carbonate-silicate mixing lithology to give a further understanding of basin scale chemical weathering estimation.

The Pearl River located in the subtropical area in South China includes three principal rivers: the Xijiang, Beijiang, and Dongjiang Rivers. The warm and wet climatic conditions make the pearl river a hyperactive region in China. The three river basins have distinct geological conditions. The Xijiang River is characterized as the carbonate-dominated area and the Dongjiang River has silicate as the main rock type. While the Beijiang River, which is the second largest tributary of the Pearl River, is characterized as a typical carbonate-silicate mixing basin. In addition, as the serve acid deposition (Larssen et al., 2006) and active mining area (Li et al., 2019), chemical weathering induced by sulfuric acid make the temporary and net sink of atmospheric CO_2 to be reevaluated. So that, in this study, the Beijiang River as the hyperactive region in Southeast China with a typical subtropical monsoon climate and carbonate-silicate mixing geologic settings was selected as the study area. Three main objectives are summarized as follows: (1) reveal spatial-temporal variations of major element chemistry of the river water, (2) calculate the chemical weathering rate and unravel

https://doi.org/10.5194/bg-2019-310
Preprint. Discussion started: 13 November 2019

the controlling factors on chemical weathering processes, and (3) determinate the temporary sink of CO_2 and evaluate the influence of sulfide oxidation on net sink of CO_2 by DIC apportionment procedure.

2 Study area

The Beijiang River Basin, which is the second largest tributary of the Pearl River Basin, is located in the southeast of China (Fig. 1). It covers a basin of 52 068 km^2 and has a total length of 573 km. The river basin is located in subtropical monsoon climate zone, with the mean annual temperature across the drainage basin ranging from 14°C to 22°C, the mean annual precipitation ranging from 1390 mm to 2475 mm. The average annual runoff is 51 billion m^3, with 70%-80% of the flux occurring from April to September. This can be attributed to the fact that more than 70% of the annual precipitation (about 1800 mm $year^{-1}$) is concentrated in the wet season (April to September).

Lithology in the river basin are composed of limestone, sandstone, gneiss and glutenite. In the upper basin, carbonate rock (mainly of limestone) outcrops in the west and center, while sandstone of Devonian era and mudstone of Paleogene era outcrop in the east of upper stream. In the middle of basin, limestone and sandstone cover most of the area, and Cretaceous volcanic rocks are found in the tributary (Lianjiang River), mainly granite. In the lower basin, Achaen metamorphic rocks outcrop in the west, and are composed of gneiss and schist, sandstone covers rest of area of the lower basin. Quaternary sediments scatter along the main stream of the river. The carbonate and silicate rock outcrops in the Beijiang River Basin was 10737 km^2 (28%) and 24687 km^2 (65%), respectively.

https://doi.org/10.5194/bg-2019-310
Preprint. Discussion started: 13 November 2019

Biogeosciences
Discussions
Open Access
EGU

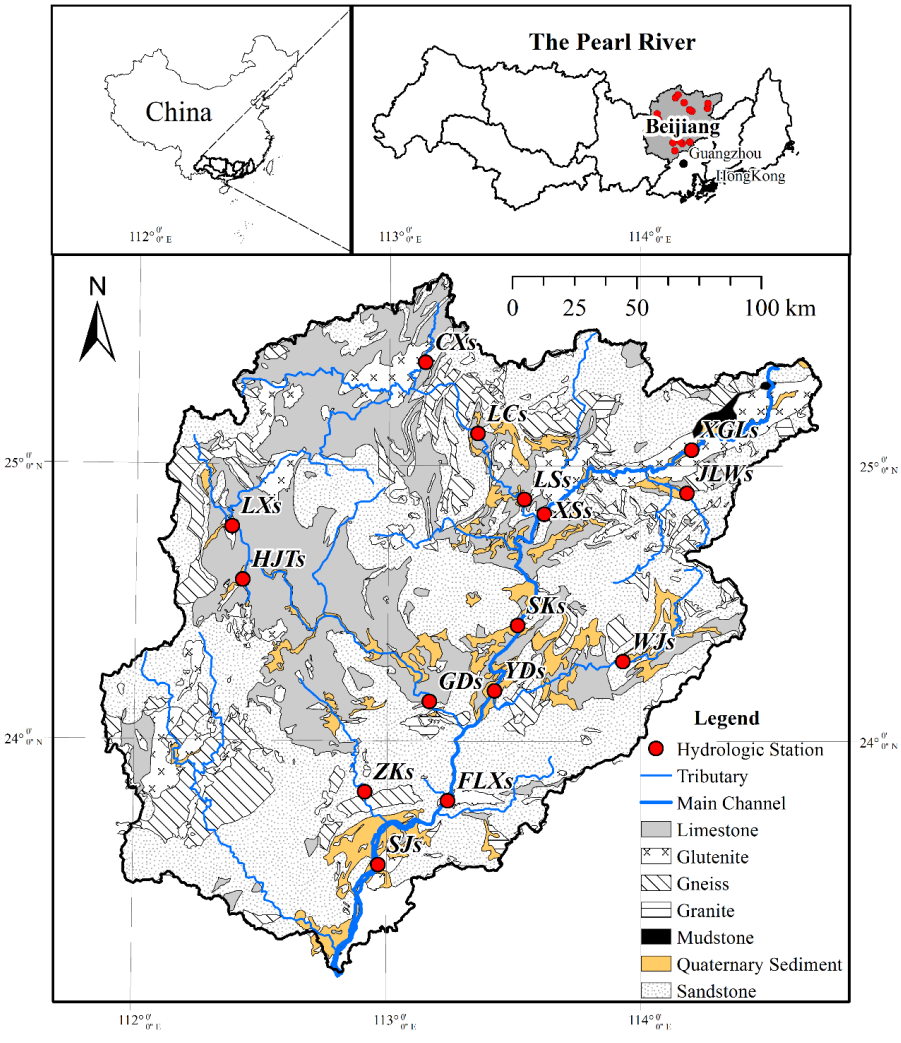

Fig. 1 Geology map and sampling point in the Beijiang River basin by ArcGis

3 Materials and methods

3.1 Sampling procedure and laboratory analysis

Water samples were collected monthly at 15 hydrologic stations from January to December in 2015 (Fig. 1). The river waters were sampled by a portable organic class water sampler along the middle thread of channel in the first day of each month. In addition, to discriminate the contribution

https://doi.org/10.5194/bg-2019-310
Preprint. Discussion started: 13 November 2019

of rain inputs, the daily rainwater was also sampled in five stations (SJs, FLXs, YDs, XSs and XGLs) along the main stream. The rainwater collector is consisted of a funnel with diameter of 20 cm and a 5 L plastic bottle. A rubber ball is setup in the funnel to prevent evaporation. All the river and rain water were filtered through 0.45 μm glass fiber filter and stored in 100 ml tubes and stored below 4°C until analysis.

Electric conductivity (EC), pH and temperature (T) were measured by a multi-parameter water quality meter (HACH-HQ40Q), and alkalinity (HCO_3^-) was measured in filtered water samples by titration in situ. The cations (Na^+, K^+, Ca^{2+}, Mg^{2+}) and anions (Cl^-, SO_4^{2-}) were analyzed by ion chromatography (ThermoFisher ICS-900) with limit of detection (L.O.D) of 0.01 mg/L. The dissolved SiO_2 was measured by molybdenum yellow method and was analyzed by ultraviolet spectrophotometer (Shimadzu UV-2600).

3.2 Calculation procedure

3.2.1 Chemical weathering rates

According to the principle of the mass balance, the mass balance equation for element *X* in the dissolved load can be expressed as (Galy and France-Lanord, 1999):

$$[X]_{\mathrm{riv}} = [X]_{\mathrm{pre}} + [X]_{\mathrm{eva}} + [X]_{\mathrm{sil}} + [X]_{\mathrm{car}} + [X]_{\mathrm{anth}} \quad (1)$$

Where $[X]$ denotes the elements of Ca^{2+}, Mg^{2+}, Na^+, K^+, Cl^-, SO_4^{2-}, HCO_3^- in $mmol \cdot L^{-1}$. The subscripts riv, pre, eva, sil, car and anth denotes the river, precipitation source, evaporite source, silicate source, carbonate source and anthropogenic source.

On the basis of the theory of rock chemical weathering and ignoring the anthropogenic origins of major ions (except for SO_4^{2-}) due to relative low TDS of river water samples (Cao et al., 2016a;

https://doi.org/10.5194/bg-2019-310
Preprint. Discussion started: 13 November 2019

Gaillardet et al., 1999b) ranged from 73.79 to 230.16 mg·L^{-1}, the major elements of river water can be simplified as followed:

$$[Cl^-]_{riv} = [Cl^-]_{pre} + [Cl^-]_{eva} \quad (2)$$

$$[K^+]_{riv} = [K^+]_{pre} + [K^+]_{sil} \quad (3)$$

$$[Na^+]_{riv} = [Na^+]_{pre} + [Na^+]_{eva} + [Na^+]_{sil} \quad (4)$$

$$[Ca^{2+}]_{riv} = [Ca^{2+}]_{pre} + [Ca^{2+}]_{sil} + [Ca^{2+}]_{car} \quad (5)$$

$$[Mg^{2+}]_{riv} = [Mg^{2+}]_{pre} + [Mg^{2+}]_{sil} + [Mg^{2+}]_{car} \quad (6)$$

$$[HCO_3^-]_{sil} = [K^+]_{sil} + [Na^+]_{sil} + 2[Mg^{2+}]_{sil} + 2[Ca^{2+}]_{sil} \quad (7)$$

$$[HCO_3^-]_{car} = [HCO_3^-]_{riv} - [HCO_3^-]_{sil} \quad (8)$$

$$[SO_4^{2-}]_{riv} = [SO_4^{2-}]_{pre} + [SO_4^{2-}]_{anth} \quad (9)$$

Firstly, the measured ion concentrations of the rain water are rectified by evaporation coefficient α=0.63=P/R (with P the precipitation and R the runoff) and calculated the contributions of atmospheric precipitation. Secondly, due to low TDS, the anthropogenic contributions are negligible. Thirdly, the molar ratios of Ca^{2+}/Na^+ (0.4) and Mg^{2+}/Na^+ (0.2) for silicate end-member (Zhang et al., 2007b) are used to calculate the contribution of Ca^{2+} and Mg^{2+} from silicate weathering, and then, residual Ca^{2+} and Mg^{2+} were attributed to carbonate weathering. For monthly data, the contributions of different sources can be calculated as followed:

$$R_{car}=([Ca^{2+}]_{car}+[Mg^{2+}]_{car})/S \times 100\% \quad (10)$$

$$R_{sil}=([K^+]_{sil}+[Na^+]_{sil}+[Ca^{2+}]_{sil}+[Mg^{2+}]_{sil})/S \times 100\% \quad (11)$$

$$R_{eva}=[Na^+]_{eva}/S \times 100\% \quad (12)$$

$$R_{pre}=([K^+]_{pre}+[Na^+]_{pre}+[Ca^{2+}]_{pre}+[Mg^{2+}]_{pre})/S \times 100\% \quad (13)$$

$$S = [Ca^{2+}]_{car} + [Mg^{2+}]_{car} + [Ca^{2+}]_{sil} + [Mg^{2+}]_{sil} + [Na^+]_{sil} + [K^+]_{sil} + [Na^+]_{eva} +$$

https://doi.org/10.5194/bg-2019-310
Preprint. Discussion started: 13 November 2019

$$[Ca^{2+}]_{pre} + [Mg^{2+}]_{pre} + [Na^{+}]_{pre} + [K^{+}]_{pre} \quad (14)$$

Where R denotes the proportions of dissolved cations from different sources. S denotes the total concentrations of cations for river water in mmol·L^{-1}.

The total, carbonate and silicate chemical weathering rates (TWR, CWR and SWR) can be estimated as followed:

$$CWR=\sum_{i=1}^{n=12}[\left(24\times[Mg^{2+}]_{car}+40\times[Ca^{2+}]_{car}+61\times[HCO_3^-]_{car}\times 0.5\right)_i\times Q_i/(10^6A)] \quad (15)$$

$$SWR=\sum_{i=1}^{n=12}[\left(39\times[K^{+}]_{sil}+23\times[Na^{+}]_{sil}+24\times[Mg^{2+}]_{sil}+40\times[Ca^{2+}]_{sil}+96\times[SiO_2]_{sil}\right)_i\times Q_i/(10^6A)] \quad (16)$$

$$TWR=CWR+SWR \quad (17)$$

Where TWR, CWR and SWR have the unit of t km^{-2} a^{-1},Q_i denotes discharge in m^3·month^{-1}, and A denotes the catchment area in km^2.

3.2.2 DIC apportionments

The riverine DIC originates from several sources including carbonate minerals, respired soil CO_2 and atmospheric CO_2, and it could be affected by processes occurring along the water pathways (Khadka et al., 2014; Li et al., 2008). Four dominant weathering processes, including (1) carbonate weathering by carbonic acid (CCW), (2) carbonate weathering by sulfuric acid (SCW), (3) silicate weathering by carbonic acid (CSW), (4) and silicate weathering by sulfuric acid (SSW), can be described by the following reaction equations:

$$CCW:(Ca_{2-X}Mg_x)(CO_3)_2 + 2H_2CO_3 \rightarrow (2-x)Ca^{2+} + xMg^{2+} + 4HCO_3^- \quad (18)$$

$$SCW:(Ca_{2-X}Mg_x)(CO_3)_2 + H_2SO_4 \rightarrow (2-x)Ca^{2+} + xMg^{2+} + 2HCO_3^- + SO_4^{2-} \quad (19)$$

$$CSW:CaSiO_3 + 2H_2CO_3 + H_2O \rightarrow Ca^{2+} + H_4SiO_4 + 2HCO_3^- \quad (20)$$

https://doi.org/10.5194/bg-2019-310
Preprint. Discussion started: 13 November 2019

$$SSW{:}CaSiO_3 + H_2SO_4 + H_2O \rightarrow Ca^{2+} + H_4SiO_4 + SO_4^{2-} \quad (21)$$

Where $CaSiO_3$ represents an arbitrary silicate.

According to the study of (Galy and France-Lanord, 1999) and (Spence and Telmer, 2005), carbonate and silicate weathering by carbonic acid in the same ratio as carbonate and silicate weathering by sulfuric acid, for monthly data the mass balance equations are followed:

$$[SO_4^{2-}]_{riv} - [SO_4^{2-}]_{pre} = [SO_4^{2-}]_{SCW} + [SO_4^{2-}]_{SSW} \quad (22)$$

$$[SO_4^{2-}]_{riv} - [SO_4^{2-}]_{pre} = \alpha_{SCW} \times [HCO_3^-]_{riv} \times 0.5 + \frac{\alpha_{CSW} \times \alpha_{SCW}}{\alpha_{CCW}} \times [HCO_3^-]_{riv} \quad (23)$$

Where the subscripts CCW, SCW, CSW and SSW denotes the four end-members defined by carbonate weathering by carbonic acid, carbonate weathering by sulfuric acid, silicate weathering by carbonic acid and silicate weathering by sulfuric acid, respectively. The parameter α denotes the proportion of DIC derived from each end-member processes.

According to the above description, the ion balance equations are followed:

$$[Ca^{2+}]_{car} + [Mg^{2+}]_{car} = \alpha_{CCW} \times [HCO_3^-]_{riv} \times 0.5 + \alpha_{SCW} \times [HCO_3^-]_{riv} \quad (23)$$

$$[SO_4^{2-}]_{SCW} + [SO_4^{2-}]_{SSW} = \alpha_{SCW} \times [HCO_3^-]_{riv} \times 0.5 + \frac{\alpha_{CSW} \times \alpha_{SCW}}{\alpha_{CCW}} \times [HCO_3^-]_{riv} \quad (24)$$

$$\alpha_{CCW} + \alpha_{SCW} + \alpha_{CSW} = 1 \quad (25)$$

Combing the above equations, the proportions of HCO_3^- derived from three end-members (CCW, SCW and CSW) can be calculated, and the DIC (equivalent to HCO_3^-) fluxes by different chemical weathering processes are calculated by following equations.

$$DIC_{CCW} = \alpha_{CCW} \times [HCO_3^-]_{riv} \quad (26)$$

$$DIC_{SCW} = \alpha_{SCW} \times [HCO_3^-]_{riv} \quad (27)$$

$$DIC_{CSW} = \alpha_{CSW} \times [HCO_3^-]_{riv} \quad (28)$$

https://doi.org/10.5194/bg-2019-310
Preprint. Discussion started: 13 November 2019


Biogeosciences Discussions Open Access EGU

3.2.3 CO_2 consumption rate and CO_2 net sink

According to the equations (17)~ (20), only the processes of CCW and CSW can consume the CO_2 from atmosphere or soil and only half of the HCO_3^- in the water due to carbonate weathering by carbonic acid come from atmospheric CO_2. Thus, the CO_2 consumption rates (CCR) for CCW and CSW can be calculated as followed (Zeng et al., 2016):

$$CCR_{CCW} = \sum_{i=1}^{n=12}\{[0.5 \times (Q/A) \times [HCO_3^-]_{CCW}]/1000\}_i \quad (29)$$

$$CCR_{CSW} = \sum_{i=1}^{n=12}\{[(Q/A) \times [HCO_3^-]_{CSW}]/1000\}_i \quad (30)$$

Where Q is discharge in $m^3 \cdot a^{-1}$, $[HCO_3^-]$ is concentration of HCO_3^- in $mmol \cdot L^{-1}$, A is catchment area in km^2. So that the CCR has the unit of 10^3 mol $km^{-2} \cdot a^{-1}$.

According to the classical view of the global carbon cycling (Berner and Kothavala, 2001), the CCW is not a mechanism that can participate to the amount of CO_2 in the atmosphere because all of the atmospheric fixed through CCW is returned to the atmosphere during carbonate precipitation in the ocean. However, when sulfuric acid is involved as a proton donor in carbonate weathering, half of the dissolved carbon re-release to the atmospheric during carbonate precipitation. Thus, SCW leads to a net release of CO_2 in ocean-atmosphere system over timescale typical of residence time of HCO_3^- in the ocean (10^5 years). Meanwhile, in case of CSW, followed by carbonate deposition, one of the two moles of CO_2 involved is transferred from the atmosphere to the lithosphere in the form of carbonate rocks, while the other one returns to the atmosphere, resulting a net sink of CO_2. Therefore, the net CO_2 consumption rate (CCR_{Net}) due to chemical weathering can be concluded as followed:

$$CCR_{Net} = \sum_{i=1}^{n=12}\{[(0.5 \times [HCO_3^-]_{CSW} - 0.5 \times [HCO_3^-]_{SCW}) \times (Q/A)]/1000\}_i \quad (31)$$

https://doi.org/10.5194/bg-2019-310
Preprint. Discussion started: 13 November 2019

3.3 Spatial and statistical analysis

The hypsometric integral value (HI) (PIKE and WILSON, 1971) was employed in this study to evaluate the influence of terrain on the chemical weathering. HI is an important index to reveal the relationship between morphology and development of landforms and can be used to establish the quantitative relationship between the stage of geomorphological development and the material migration in the basin (PIKE and WILSON, 1971; Singh et al., 2008; STRAHLER, 1952). The HI value of each watershed is calculated by the elevation-relief ratio method and can be obtained by the following equation (PIKE and WILSON, 1971):

$$\mathrm{HI} = \frac{\mathrm{Mean.elevation} - \mathrm{Min.elevation}}{\mathrm{Max.elevation} - \mathrm{Min.elevation}}$$

where HI is the hypsometric integral; Mean.elevation is the mean elevation of the watershed; Min.elevation is the minimum elevation within the watershed; Max.elevation is the maximum elevation within the watershed. According to the hypsometric integral value (HI), the geomorphological development can be divided into three stages: inequilibrium or young stage (HI > 0.6), equilibrium or mature stage ($0.35 < \mathrm{HI} \leqslant 0.6$), and monadnock or old age ($\mathrm{HI} \leqslant 0.35$), which can reflect the erodible degree and erosion trend of the geomorphology (Xiong et al., 2014).

The watershed of the study area was divided by using hydrological analysis module of ArcGIS. The average slope and HI was conducted by spatial analysis module of ArcGIS. All statistical tests were conducted using SPSS version 22.0. One-way analysis of variance (ANOVA) was performed for differences of monthly major ion concentrations and dissolved inorganic carbonate isotopes with significance at $p<0.05$. Principal component analysis (PCA) was employed to unravel the underlying data set through the reduced new variables, analyzed the significant factors affecting the characteristics of water chemistry.

https://doi.org/10.5194/bg-2019-310
Preprint. Discussion started: 13 November 2019

4 Results

4.1 Chemical composition in the Beijiang River Basin

The major physical-chemical parameters of river water samples were presented in Table 1. For all the monthly samples, the pH values ranged from 7.5 to 8.5 with an average of 8.05. Average electrical conductivity was 213 $\mu s \cdot cm^{-1}$, ranging from 81 to 330 $\mu s \cdot cm^{-1}$. The TDS of river water samples varied from 73.8 to 230.2 $mg \cdot L^{-1}$, with an average of 157.3 $mg \cdot L^{-1}$, which was comparable with the global average of 100 $mg \cdot L^{-1}$ (Gaillardet et al., 1999a). Compared with the major rivers in China, the average TDS was significantly lower than the Changjiang (Chen et al., 2002b) , the Huanghe (He Jiangyi, 2017) the Zhujiang (Zhang et al., 2007b), the Huaihe (Zhang et al., 2011) and the Liaohe (Ding et al., 2017). However, the average TDS was higher than the rivers draining silicate-rock-dominated areas, e.g., Dojiang River (59.9 $mg \cdot L^{-1}$) in Southern China (Xie chenji, 2013), North Han River (75.5 $mg \cdot L^{-1}$) in South Korea, (Ryu et al., 2008), the Amazon (41 $mg \cdot L^{-1}$) and the Orinoco (82 $mg \cdot L^{-1}$) draining the Andes (Dosseto et al., 2006; Edmond et al., 1996).

258 **Table 1 The major physical-chemical parameters of river water samples at 15 hydrological station in the Beijiang River (mean±SD). The total dissolved solid (TDS,**

259 **mg·L^{-1}) expressed as the sum of major inorganic species concentration (Na^++K^++Ca^{2+}+Mg^{2+}+HCO_3^-+Cl^-+SO_4^{2-}+NO_3^-+SiO_2)**

Hydrological stations	pH	EC (μs/cm)	TDS (mg/L)	Na^+ (μmol/L)	K^+ (μmol/L)	Ca^{2+} (μmol/L)	Mg^{2+} (μmol/L)	HCO_3^- (μmol/L)	Cl^- (μmol/L)	SO_4^{2-} (μmol/L)	SiO_2 (μmol/L)	HI
JLWs	7.9±0.15	95±39.98	81.1±25.6	111.4	51.9	223.5	103.9	701.9	28.3	44.5	225.2	0.3444
CXs	8.2±0.15	219±50.32	163.7±20.9	118.1	40.1	793.3	187.1	1593.6	60.5	199.4	106.3	0.2865
HJTs	8.1±0.19	203±34.39	151.8±21.9	100.2	29.9	686.7	203.9	1708.7	29.5	72.2	156.6	0.2991
ZKs	8.1±0.13	218±44.84	161.3±21.1	426.4	66.2	560.3	134.1	1276.9	134.7	161.4	151.9	0.2233
XGLs	7.8±0.15	168±15.83	117.9±8.9	315.4	112.4	422.4	101.0	992.2	213.9	112.6	178.9	0.1821
WJs	8.1±0.1	260±26.91	172.9±16.7	197.8	59.0	767.3	122.6	1467.1	99.1	162.8	183.4	0.2462
LXs	8.1±0.16	236±32.99	171.8±19.6	122.1	38.1	813.5	176.0	1829.4	51.5	89.2	145.7	0.2149
LCs	8.2±0.09	253±25.91	196.1±20.0	287.4	46.8	862.6	234.4	1845.7	115.7	232.4	130.7	0.2731
LSs	8.3±0.06	220±45.62	184.2±18.3	258.9	58.2	793.5	202.9	1740.6	109.0	191.9	121.4	0.2503
XSs	7.9±0.14	156±29.8	123.9±17.6	305.0	86.1	366.8	110.9	966.6	103.8	166.5	218.7	0.2365
GDs	8.1±0.05	232±10.67	169.4±8.3	112.6	40.5	781.6	172.1	1798.5	44.0	90.3	141.2	0.2415
SKs	8.1±0.19	238±21.6	161.1±17.4	345.3	73.6	641.0	162.5	1304.1	174.4	223.5	160.1	0.2061
Yds	7.8±0.2	241±54.39	165.9±34.0	296.4	59.3	674.8	160.9	1515.0	118.7	175.9	144.4	0.2055
FLXs	8±0.21	232±36.99	161.4±22.8	187.6	95.1	577.0	135.0	1262.4	111.9	159.6	169.5	0.2065
SJs	8.1±0.1	230±26.94	176.4±18.9	355.0	83.4	663.5	156.2	1367.7	182.4	190.5	180.5	0.2057

260

https://doi.org/10.5194/bg-2019-310
Preprint. Discussion started: 13 November 2019

261 Major ion composition were shown in the anion and cation ternary diagrams (Fig. 2). Ca^{2+} was
262 the dominant cation with concentration ranging from 199 to 1107 μmol·L^{-1}, accounting for
263 approximately 49% to 81%, with an average of 66% (in μEq) of the total cation composition in the
264 river water samples. HCO_3^- was the dominant anion, with concentration ranging from 640 to 2289
265 μmol·L^{-1}. On average, it comprised 77% (59%~92%) of total anions, followed by SO_4^{2-} (16%) and
266 Cl^- (6%). The major ionic composition indicated that the water chemistry of the Beijiang River
267 Basin was controlled by both carbonate and silicate weathering.

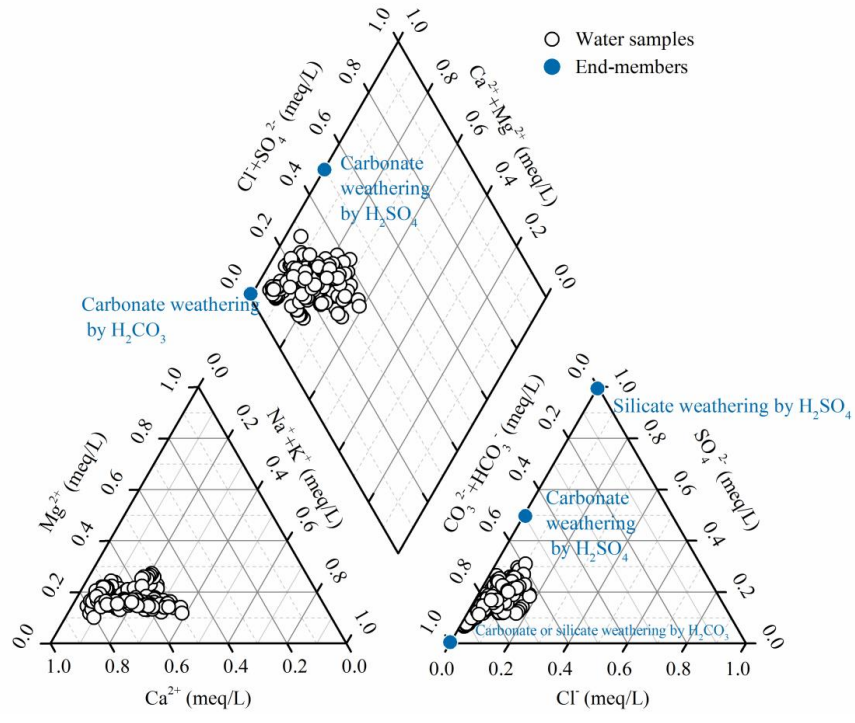

268

269 **Fig. 2 Piper diagram of river water samples in the Beijiang River**

270 The principal component analysis (PCA) was used to study the factors controlling the chemical
271 compositions. The varimax rotation was used to reduced the number of variables to two principal
272 components (PCs), which together explain 76.88% of the total variance in the data. The first PC

https://doi.org/10.5194/bg-2019-310
Preprint. Discussion started: 13 November 2019

(PC1) explained approximately 50.02% of the total variations, and was considered to represent "carbonate weathering factor" because of the high contributions of EC, TDS, Ca^{2+}, Mg^{2+} and HCO_3^- concentrations. The second PC (PC2) explained 26.85% of the total variance and presented high loadings for Na^+ and K^+ concentrations. Thus, the PC2 represented an "silicate weathering factor", which were considered to be two important sources of these ions in the Beijiang River Basin (Li et al., 2019).

4.2 Seasonal and spatial variations

There were significantly seasonal variations in the major ion concentrations (Fig. 3). Two basic patterns of temporal variations could be observed. The first one was related to the carbonate weathering derived ions such as Ca^{2+} and HCO_3^-, which showed high values in Nov and low values in Jun. The second one was for the silicate weathering derived ions such as Na^+ and K^+, which showed high values in Feb and low values in Jun. The minimums occurred in Jun for all the ions showed a significant dilution effect during the high-flow periods.

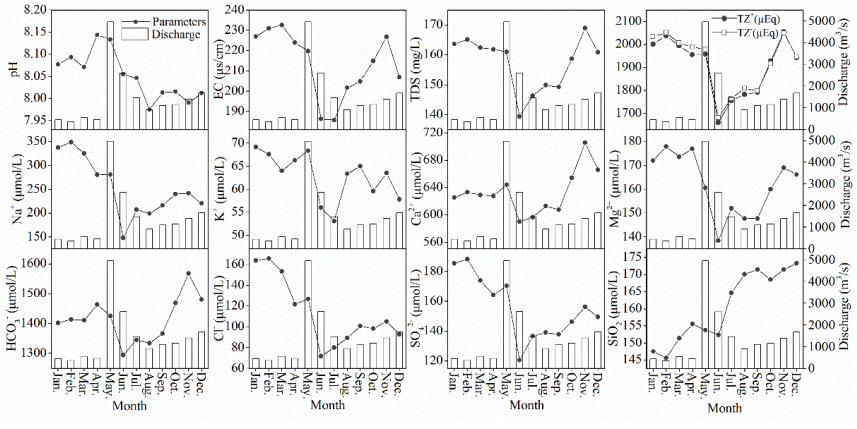

Fig. 3 Monthly variations of environmental parameters and major ion concentrations in the Beijiang River Basin (SJs station). The columns denoted the monthly discharge

https://doi.org/10.5194/bg-2019-310
Preprint. Discussion started: 13 November 2019

289 It is clear that the Ca^{2+} and HCO_3^- concentrations had a decreasing trend from upstream to
290 downstream (Fig. 4), this characteristic agrees with the trends observed in the Changjiang River and
291 the Huai River, where the major elements or TDS concentrations of the main channel showed a
292 general decreasing trend, and the tributaries display the dilution effect to the main channel. For other
293 silicate weathering derived ions such as Na^+, there was a slight increasing trend implying the
294 chemical inputs from the tributaries. These trends were in accordance with the lithology in the study
295 area. The carbonate is dominated in the upper stream basin, when river drainages this area, carbonate
296 weathering contributes to the elevation of Ca^{2+} and HCO_3^-. As the river entered into the down stream
297 dominated with silicate, the relative low ion concentrations due to silicate weathering contributed
298 to dilute the Ca^{2+} and introduce extra Na^+ in the river.

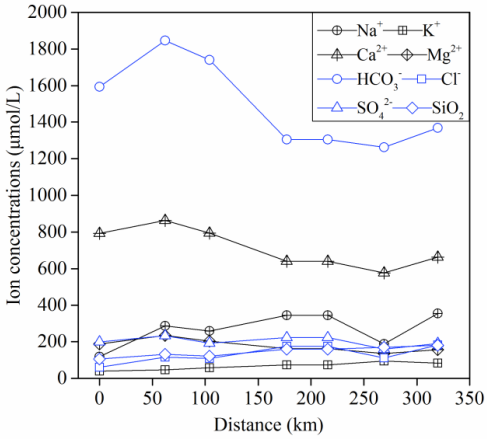

299

300 **Fig. 4 Spatial variations of major ion and SiO_2 concentrations in the Beijiang River Basin (From**
301 **upstream station CXs to the downstream station SJs)**

https://doi.org/10.5194/bg-2019-310
Preprint. Discussion started: 13 November 2019

5 Discussion

5.1 Chemical weathering rates and the controlling factors

5.1.1 Chemical weathering rates

Atmospheric precipitation inputs, anthropogenic inputs and chemical weathering of rocks and minerals as the major sources contributed to the hydrochemistry in the river basin. Previous studies have shown that rock weathering contributions to major element composition of the river can be interpreted in terms of mixing between three main end-members corresponding to the weathering products of carbonates, silicates and evaporates (Cao et al., 2016b; Négrel et al., 1993; Ollivier et al., 2010). The river water samples in the Beijiang River Basin were displayed on the plots of Na-normalized molar ratios (Fig. 5). The best correlations were observed between Ca^{2+}/Na^{+} and Mg^{2+}/Na^{+} (R^2=0.86, n=180) and Ca^{2+}/Na^{+} and HCO_3^{-}/Na^{+} (R^2=0.96, n=180). In these plots, the contributions from carbonate weathering correspond to the trend toward high-Ca^{2+} end-member close to the top right corner, while silicate weathering correspond to the trend toward to high-Na^{+} end-member close to the low-left corner. It was clear that the samples with high ratio of carbonate outcrop had the highest molar ratios of Ca^{2+}/Na^{+}, Mg^{2+}/Na^{+} and HCO_3^{-}/Na^{+}, which made the samples located toward to the carbonate weathering end-member. However, the samples with low Ca^{2+}/Na^{+}, Mg^{2+}/Na^{+} and HCO_3^{-}/Na^{+} ratios showed the influence of silicate weathering. In addition, major ion compositions of the Beijiang River was mainly contributed by the weathering of carbonates and silicates, and showed little contribution of evaporate weathering.

https://doi.org/10.5194/bg-2019-310
Preprint. Discussion started: 13 November 2019

Biogeosciences
Discussions
Open Access
EGU

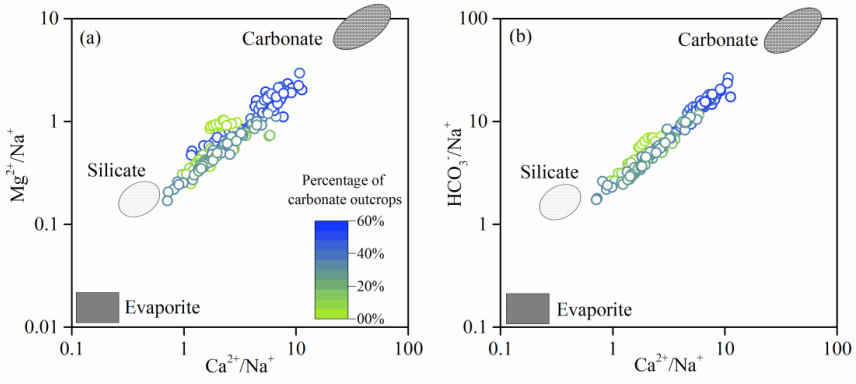

Fig. 5 Mixing diagrams using Na-normalized molar ratios: (a) Mg^{2+}/Na^{+} vs. Ca^{2+}/Na^{+} (b) HCO_3^{-}/Na^{+} vs. Ca^{2+}/Na^{+} for the Beijiang River Basin. The color ramp showed the percentage of carbonate outcrops

Based on the chemical balance method, the calculated contributions of different sources to the total cationic loads were presented in Fig. 6. The results showed that carbonate weathering was the most important mechanism controlling the local hydrochemistry, and contributed approximately 50.06% (10.96%~79.96%) of the total cationic loads. Silicate weathering and atmospheric precipitation inputs accounted for 25.71% (5.55%~70.38%) and 17.92% (0~46.95%), respectively. Evaporate weathering had the minimum contribution with an average of 6.31% (0~24.36%) to the total cationic loads.

https://doi.org/10.5194/bg-2019-310
Preprint. Discussion started: 13 November 2019

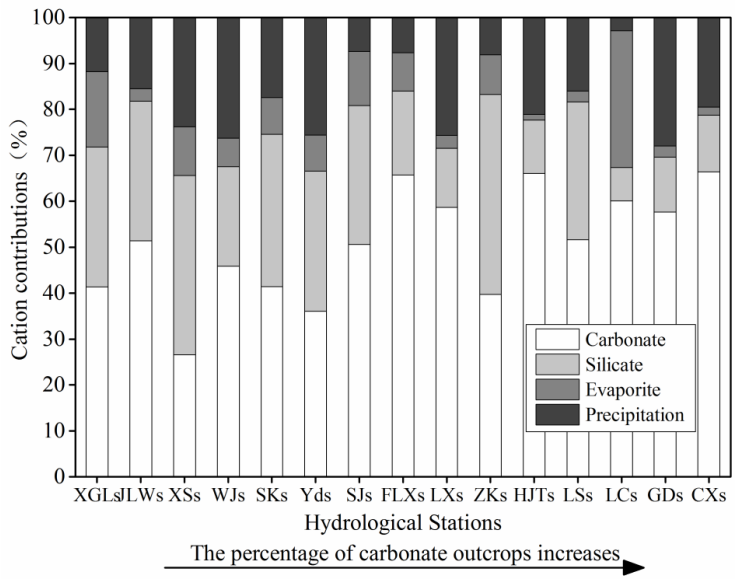

Fig. 6 Calculate contributions (in %) from the different hydrological stations to the total cationic load in the Beijiang River Basin. The cationic loads were the sum of Na^+, K^+, Ca^{2+} and Mg^{2+}

The chemical weathering rates were calculated and the results were listed in Table 2. The average of carbonate and silicate weathering rate in the Beijiang River Basin were 61.15 and 25.31 $t \cdot km^{-2} \cdot a^{-1}$, respectively. In addition, chemical weathering rates showed significantly seasonal variations with the highest carbonate and silicate weathering rates in May (16.75 and 5.50 $t \cdot km^{-2} \cdot month^{-1}$, respectively) and the lowest carbonate and silicate weathering rates in February (0.95 and 0.39 $t \cdot km^{-2} \cdot month^{-1}$, respectively). (Gaillardet et al., 1999a) reported the chemical weathering rate of major river all over the world. The summarized dataset was showed in Fig. 7. It is found that the hyperactive zone with high chemical weathering rate is generally located between the latitude 0-30° and our study is belong to this area. Average CWR and SWR were about 61.15 and 25.31 $t \cdot km^{-2} \cdot month^{-1}$, respectively. The carbonate weathering contribute about 70% of the total chemical weathering. The factors influence the balance between CWR and SWR would be further discussed

https://doi.org/10.5194/bg-2019-310
Preprint. Discussion started: 13 November 2019

346 in the following parts.

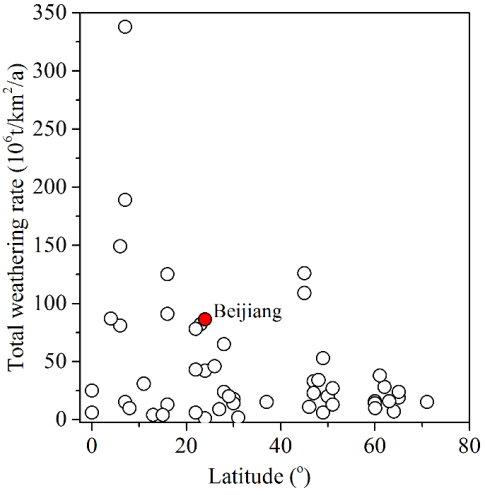

347

348 **Fig. 7 Relationship between latitude and total weathering rate (TWR)**

349

350 **Table 2 The annual discharge, catchment area, carbonate and silicate outcrops proportions, and**

351 **calculated weathering rates of carbonate and silicate of 15 subcatchments in the Beijiang River**

ID	Annual discharge (10^8m^3/a)	Catchment area (km^2)	Percentages of carbonate (%)	Percentages of silicate (%)	Carbonate weathering rate -CWR (t km^{-2} year^{-1})	Silicate weathering rate -SWR (t km^{-2} year^{-1})	Total weathering rate -TWR (t km^{-2} year^{-1})
JLWs	2.23	281.13	2.95	97.05	18.63	14.94	33.56
CXs	4.06	392.35	57.44	42.56	74.21	11.42	85.64
HJTs	11.54	503.02	41.99	55.83	169.12	29.73	198.85
ZKs	16.38	1655.22	34.60	61.81	35.03	24.14	59.17
XGLs	13.56	1863.02	0.38	93.07	25.75	13.96	39.72
WJs	19.11	1960.99	12.51	73.87	55.00	17.43	72.43
LXs	56.37	2458.06	34.32	64.07	178.71	29.39	208.10
LCs	58.74	5278.14	49.67	50.21	79.70	20.59	100.29
LSs	74.83	6994.69	44.59	52.44	69.28	14.94	84.22
XSs	62.11	7497.01	7.09	87.81	18.85	20.35	39.20
GDs	137.81	9028.38	49.93	44.93	111.73	19.19	130.92
SKs	49.51	17417.24	25.43	69.35	12.71	6.11	18.82
YDs	191.07	18234.64	25.63	68.05	52.37	19.59	71.95

https://doi.org/10.5194/bg-2019-310
Preprint. Discussion started: 13 November 2019

FLXs	396.25	34232.34	29.68	63.49	68.38	17.53	85.91
SJs(Average)	450.90	38538.06	28.12	64.65	61.15	25.31	86.46

352

353 **5.1.2 Factors affecting chemical weathering**

354 Many factors control the chemical weathering rates within river basins, including terrain,
355 geotectonic properties, lithology, land cover, climatic conditions (temperature, precipitation, etc.),
356 and hydrological characteristics (Ding et al., 2017; Gislason et al., 2009; Hagedorn and Cartwright,
357 2009). For this study, the lithology, hydrological characteristics and geomorphology was selected
358 as the major factors to be discussed.

359 **5.1.2.1 Lithology**

360 Among all the factors controlling the chemical weathering rates, lithology is one of the most
361 important factors because different type of rocks have different weathering abilities (Viers et al.,
362 2014). The TWR had a significant positive correlation (p<0.01) with the ratios of the proportion of
363 carbonate and a non significant positive correlation with that of silicate outcrops (Fig. 8a, b). Further
364 more, a significant correlation (p<0.01) was found between the CWR and proportion of carbonate
365 outcrops (Fig. 8c), but the correlations between the SWR and the proportion of silicate outcrops
366 were low and not statistically significant (p>0.05, Fig. 8d). The correlation analysis confirmed that
367 carbonate outcrops ratios was the sensitive factor controlling the chemical weathering rates and the
368 rapid kinetics of carbonate dissolution played an important role in weathering rates in the Beijiang
369 River Basin.

https://doi.org/10.5194/bg-2019-310
Preprint. Discussion started: 13 November 2019

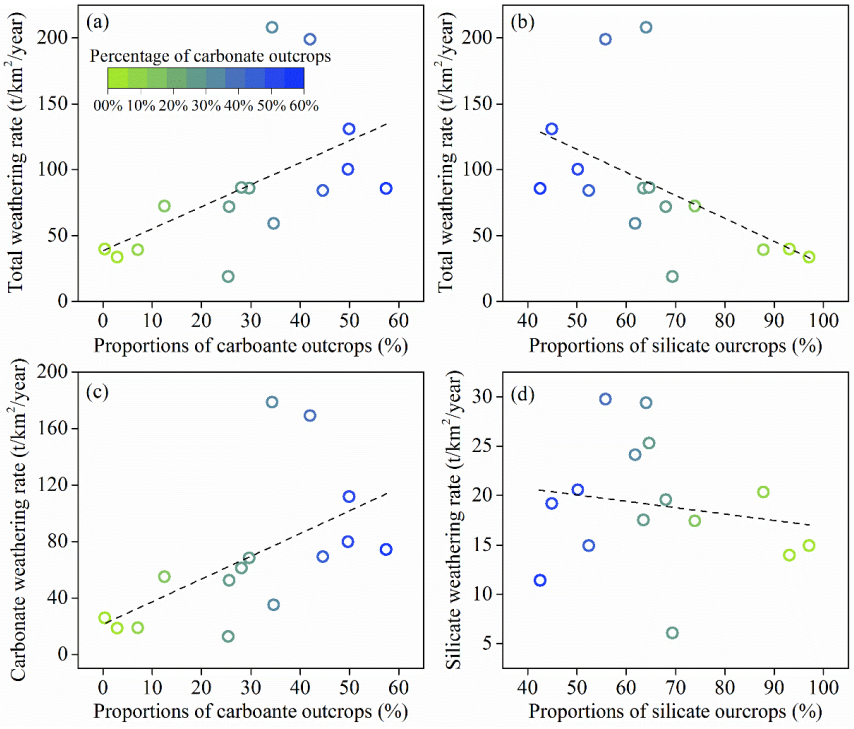

Fig. 8 The relationships between weathering rates and the proportions of carbonate or silicate outcrops

5.1.2.2 Runoff

Chemical weathering is a combination of two processes, including dissolution of primary minerals/glasses and precipitation of secondary minerals/biota growth (Eiriksdottir et al., 2011; Hartmann et al., 2014a; Liu et al., 2013). The dissolution process is quite related to the precipitation and runoff. In general, river water chemistry is usually diluted by river runoff (Q), and this dilution effect is variable in different basins (Rao et al., 2019). The dilution effects of major element caused by increasing water flow can be expressed by following log linear equation, the standard rating relationship (Li et al., 2014; Walling, 1986; Zhang et al., 2007a):

$$C_i = aQ^b$$

https://doi.org/10.5194/bg-2019-310
Preprint. Discussion started: 13 November 2019

where C_i is the concentration of element i (mmol/L), Q is the water discharge (m^3/s), a is the regression constant and b is the regression exponent. The linear fitting result was showed by Fig. 9 and the parameters b for major elements obtained from the dataset were 0.08 (Na^+), 0.05 (K^+), 0.08 (Ca^{2+}), 0.02 (Mg^{2+}), 0.06 (HCO_3^-), 0.12 (Cl^-), 0.11 (SO_4^{2-}) and -0.005 (SiO_2), respectively. In many cases, b ranges from -1 to 0 due to the chemical variables that are influenced in various ways and various extents. However, in our study area, the values of b were positive and not comparable to the observations in the major Asian River such as the Yangtze (Chen et al., 2002a), the Yellow (Chen et al., 2005), the Pearl Rivers (Zhang et al., 2007a) and the Mekong River (Li et al., 2014). This suggests additional and significant solute sources in the river basin that may contribute and compensate considerably the effect of dilution by precipitation. The difference of slope for individual dissolved components at different stations reflects the different sources and the solubility of source materials.

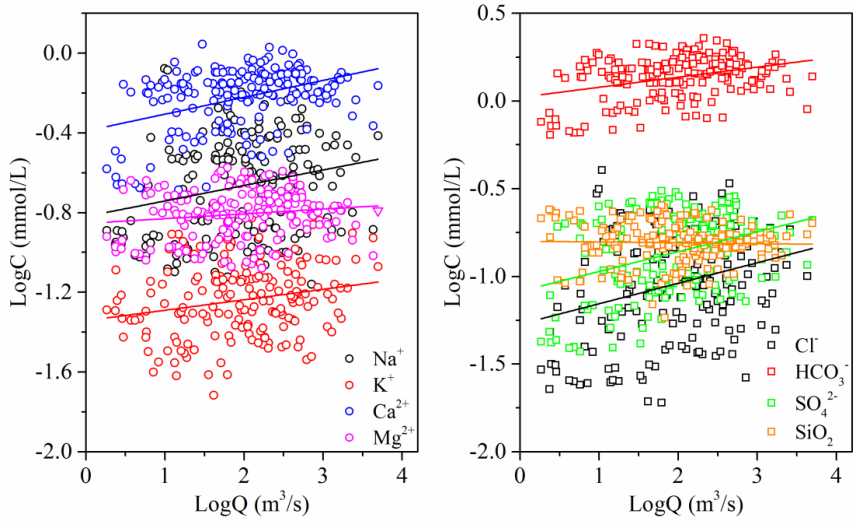

Fig. 9 The relationship between major ion concentrations and runoff (Q) in logarithmic scales

Due to the compensation effect of chemical weathering, significant positive linear relationship

https://doi.org/10.5194/bg-2019-310
Preprint. Discussion started: 13 November 2019

397 was detected between Q and TWR, CWR and SWR. So that, the linear regression analysis between
398 Q and TWR, CWR and SWR were conducted to further reveal the effect of runoff on chemical
399 weathering rate. The slope of the liner regression equations for all 15 hydrological station
400 watersheds in the Beijiang River Basin were summarized in Table 3. The linear relations indicated
401 that the increase of runoff could accelerate the chemical weathering rates, but the variations of K
402 values revealed that the degrees of influences were different due to multiple factor influence, such
403 as the influence of geomorphology.

404 **Table 3 The slope of the liner regression equation between runoff (Q) and total weathering rate**
405 **(TWR), carbonate weathering rate (CWR) and silicate weathering rate (SWR)**

Hydrological stations	Total weathering rate $=K_1Q$		Carbonate weathering rate $=K_2Q$		Silicate weathering rate $=K_3Q$	
	K_1	R^2	K_2	R^2	K_3	R^2
JLWs	0.3912	0.9983	0.2091	0.9962	0.1821	0.9993
CXs	0.6492	0.9335	0.5631	0.9250	0.0860	0.9378
HJTs	0.5117	0.9689	0.4421	0.9613	0.0695	0.9939
ZKs	0.0953	0.9679	0.0525	0.7612	0.0429	0.8037
XGLs	0.0835	0.9781	0.0558	0.9741	0.0278	0.9817
WJs	0.1017	0.9985	0.0842	0.9965	0.0175	0.8835
LXs	0.0968	0.9816	0.0843	0.9778	0.0125	0.9914
LCs	0.0486	0.8983	0.0401	0.8672	0.0085	0.9739
LSs	0.0359	0.9654	0.0286	0.9570	0.0073	0.9423
XSs	0.0180	0.9806	0.0080	0.9681	0.0100	0.9571
GDs	0.0252	0.9969	0.0216	0.9974	0.0036	0.9900
SKs	0.0116	0.9802	0.0083	0.9822	0.0033	0.9547
Yds	0.0106	0.9963	0.0081	0.9936	0.0026	0.9240
FLXs	0.0050	0.9681	0.0039	0.9485	0.0010	0.9949
SJs	0.0053	0.9883	0.0037	0.9706	0.0016	0.9778

406

https://doi.org/10.5194/bg-2019-310
Preprint. Discussion started: 13 November 2019

5.1.2.3 Geomorphology

The geomorphology factors including catchment area, average slope and HI, which could quite influence the runoff generation process and physical and chemical weathering, were selected to give a further explanation of the variation of K values. As showed in Fig. 10a, the K values were found a non-linear relationship with the areas of subcatchment and could be fitted by exponential decay model, which showed that the K values decreased dramatically with the initial increasing of area and quickly become stable after reaching the threshold. The threshold value for K_1, K_2 and K_3 was about 5278 km^2. It indicated that the compensation effect was more significant in small catchment.

The average topographic slope of each subcatchment ranged from 37° to 63°. With the increasing of average slope, the residence time of both surface water and groundwater decrease. Kinetics of carbonate and silicate reactions were determined by the reaction time which could be related by the residence time of water. In our study area, the K values showed non-linear negative correlation with average slope (Fig. 10e, f, g). When the average slope increase, the resulted small residence time (time of water-rock reactions) make the compensation effect also weak in the study area.

Hypsometric analysis showed that the HI ranged from 0.18 to 0.34. According to the empirical classification by HI ($HI > 0.6$, inequilibrium or young stage, $0.35 < HI \leq 0.6$, equilibrium or mature stage, $HI \leq 0.35$, monadnock or old age), the geomorphological development in the Beijiang River was recognized as the old age, which reflect the erodible degree and erosion trend of the geomorphology was high. Furthermore, the non-linear positive correlations between HI and K values (Fig. 10g, h, i) also addressed that geomorphology development have significant influence on chemical weathering and relating CO_2 consumption processes.

https://doi.org/10.5194/bg-2019-310
Preprint. Discussion started: 13 November 2019

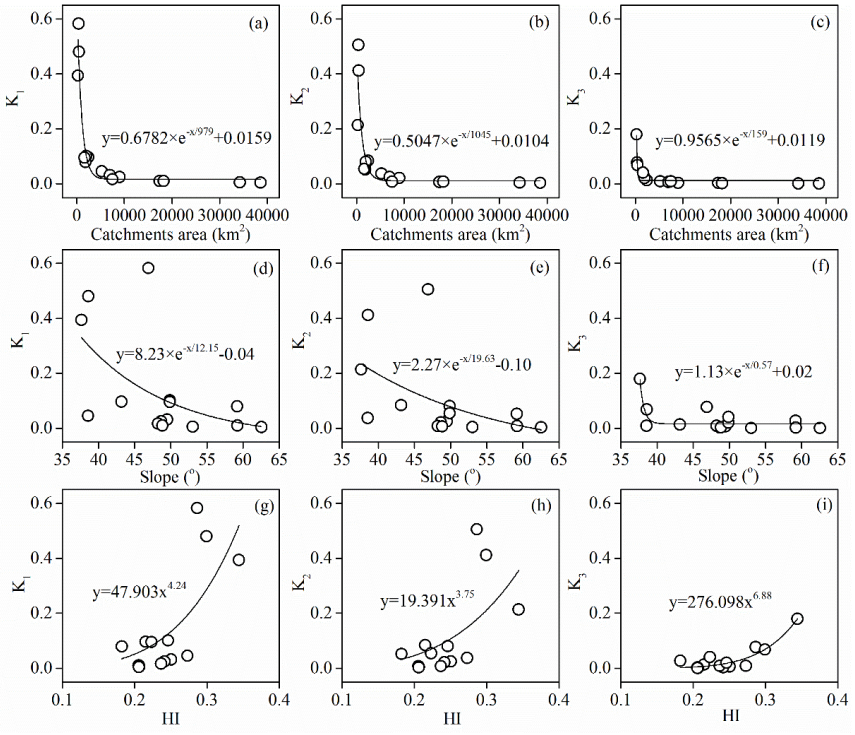

Fig. 10 The relationships between K values and catchments area (a, b, c), average slope (d, e, f) and HI (g, h, i) for the Beijiang River.

5.2 Temporary and net sink of atmospheric CO_2

5.2.1 Sulfate origin and DIC apportionment

The successful application of DIC apportionment calculation mentioned in section 3.22 is based on the sources of sulfate (SO_4^{2-}). Three sources of SO_4^{2-} should be discriminated including atmospheric acid deposition (Larssen and Carmichael, 2000), acid mining discharge (AMD) (Li et al., 2018; Li et al., 2019) and chemical weathering of evaporite such as the dissolution of gypsum (Appelo and Postma, 2005). Acid rain events occurred frequently in South and East China after 1980 (Larssen et al., 2006). The pH isolines based on data from 86 monitoring stations (Larssen et al., 2006) showed that in the Beijiang River the rain pH was lower than 4.5 and our monitoring

https://doi.org/10.5194/bg-2019-310
Preprint. Discussion started: 13 November 2019

441 dataset also proved this result. Sulfur wet deposition estimated based on the observed bulk wet sulfur
442 deposition data and the RAINS-Asia model (Larssen and Carmichael, 2000) ranged from 2000-
443 5000 eq ha^{-1} a^{-1}, which showed that the acid sulfur deposition was one of the most important sources
444 of river sulfate. In addition, considering the abundant ore resources in the Beijiang River, the second
445 possible source of SO_4^{2-} is sulfide oxidation due to mining. In our previous study, the SO_4^{2-} with
446 AMD origin mainly came from the tributary Wenjiang River (Wen et al., 2018). These two sources
447 could offer sufficient chemical weathering agent H_2SO_4 and actively involved in the chemical
448 weathering due to the following reaction mechanism (take carbonate for example) (Taylor et al.,
449 1984; van Everdingen and Krouse, 1985).

450 $$FeS_2 + \frac{7}{2}O_2 + H_2O = Fe^{2+} + 2SO_4^{2-} + 2H^+$$

451 $$2CaCO_3 + H_2SO_4 = 2Ca^{2+} + 2HCO_3^- + SO_4^{2-}$$

452 The third source came from dissolution of gypsum could not offer active H_2SO_4 to induce
453 carbonate and silicate dissolution. Two evidence were summarized to indicate the absence of
454 gypsum in the study area, (1) Lithology in the river basin are composed of limestone, sandstone,
455 gneiss and glutenite. HI showed that geomorphology development have entered into the "old" age,
456 the evaporite such halite and gypsum have been consumed by the dissolution. (2) The stoichiometric
457 relationship between Ca^{2+} and SO_4^{2-} (Fig. 11) showed that all of the samples in the study area located
458 below the 1:1 gypsum dissolution line, and due to the dissolution of carbonate, they also below the
459 1:2 carbonate weathering induced by sulfuric acid (SCW) line. These two points combined gave the
460 evidence to prove the absence of contribution of gypsum dissolution to river SO_4^{2-}. So that, the DIC
461 apportionment could be calculated according to equation (18) to (21) and the result of three main
462 processes (CCW, CSW and SCW) contributing to the DIC origin in the Beijiang River water are

https://doi.org/10.5194/bg-2019-310
Preprint. Discussion started: 13 November 2019

showed in Table 4. It was found that CCW was the dominant origin of DIC (35%~87%) and that SCW (3%~15%) and CSW (7%~59%) were non-negligible weathering processes.

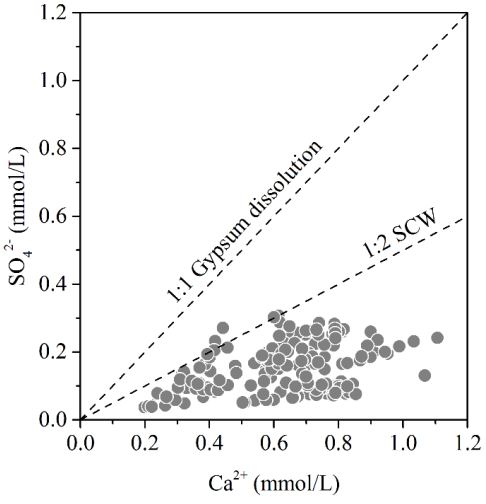

Fig. 11 Stoichiometric relationship between Ca^{2+} and SO_4^{2-}

5.2.2 Temporary and net CO_2 sink

According to the classical view of the global carbon cycling (Berner and Kothavala, 2001), the CO_2 sink induced by chemical weathering varies for different time scales. Aa short-term timescale, carbonic acid based carbonate and silicate weathering (CCW and CSW) and transport of the HCO_3^- to oceans through rivers is an important "temporary" carbon sink (Khadka et al., 2014) and can be calculated by the sum of CCR_{CCW} and CCR_{CSW}. Thus, it was significant to estimate the CCR of CCW and CSW (Liu and Dreybrodt, 2015; Liu et al., 2011). However, at the geological timescale (>10^6 years), when over the timescale typical of residence time of HCO_3^- in the ocean (10^5 years), the CCW is not a mechanism that can participate in the net sink of CO_2 in the atmosphere because all of the atmospheric CO_2 fixed through CCW is returned to the atmosphere during carbonate precipitation in the ocean. Meanwhile, in case of CSW, followed by carbonate deposition,

https://doi.org/10.5194/bg-2019-310
Preprint. Discussion started: 13 November 2019

one of the two moles of CO_2 involved is transferred from the atmosphere to the lithosphere in the form of carbonate rocks, while the other one returns to the atmosphere. The CSW is recognized as the net sink of atmosphere CO_2. In addition, when sulfuric acid is involved as a proton donor in carbonate weathering, half of the carbon dissolved to the atmospheric during carbonate precipitation. Thus, SCW leads to a net release of CO_2 in ocean-atmosphere system. So that, the net CO_2 sink (expressed by CCR_{Net} in this study) is controlled by the DIC apportionment according to equation (31).

The result of CCR_{Total}, CCR_{CCW}, CCR_{CSW} and CCR_{Net} were summarized in Table 4. The CCR_{Total} was 823.41 10^3 mol km^{-2} a^{-1}. Comparing with other Chinese rivers, such as the Songhua River (189×10^3 mol km^{-2} a^{-1}) (Cao et al., 2015) and other rivers calculated by (Gaillardet et al., 1999a) including the Heilong River (53×10^3 mol km^{-2} a^{-1}), the Changjiang River (609×10^3 mol km^{-2} a^{-1}), the Huanghe River (360×10^3 mol km^{-2} a^{-1}), the Xijiang River (960×10^3 mol km^{-2} a^{-1}), the Jinshajiang River (420×10^3 mol km^{-2} a^{-1}), the Langcangjiang River (980×10^3 mol km^{-2} a^{-1}), the Nujiang River (1240×10^3 mol km^{-2} a^{-1}), the Yalongjiang River (870×10^3 mol km^{-2} a^{-1}), the Daduhe River (1280×10^3 mol km^{-2} a^{-1}) and Minjiang River (660×10^3 mol km^{-2} a^{-1}), our study area showed relative high CCR due to high chemical weathering rate. In addition, the CCR_{CCW} and CCR_{CSW} were 536.59×10^3 (65%) and 286.82×10^3 (35%) mol km^{-2} a^{-1}, respectively. Compared with the "temporary" sink, the net sink of CO_2 for the Beijiang River was approximately 23.18×10^3 mol km^{-2} a^{-1} of CO_2 sinking in the perspective of global carbon cycling. It was about 3% of the "temporary" CO_2 sink. Human activities (sulfur acid deposition and AMD) dramatically decreased the CO_2 net sink and even make chemical weathering a CO_2 source to the atmosphere.

Table 4 Calculated CO_2 consumption rate and net sink of 15 nested subcatchments in the

https://doi.org/10.5194/bg-2019-310
Preprint. Discussion started: 13 November 2019

500 **Beijiang River Basin**

Hydrological stations	DIC apportionment (10^9 mol/a)			"Temporary" Sink (CO_2 consumption rate) (10^3 mol km^{-2} a^{-1})			Net Sink (10^3 mol km^{-2} a^{-1})
	CCW	SCW	CSW	CCR_{CCW}	CCR_{CSW}	CCR_{Total}	CCR_{Net}
JLWs	0.10	0.00	0.05	175.23	191.14	366.36	87.73
CXs	0.57	0.04	0.05	732.05	118.18	850.23	13.18
HJTs	1.57	0.06	0.34	1563.64	683.41	2247.05	286.14
ZKs	1.24	0.16	0.73	375.23	439.77	815.00	172.27
XGLs	0.85	0.14	0.37	227.05	195.91	422.95	61.59
WJs	1.76	0.17	0.87	449.32	443.18	892.50	177.50
LXs	7.30	0.40	2.61	1485.45	1060.45	2545.91	449.09
LCs	8.07	0.86	1.92	764.32	363.41	1127.95	99.77
LSs	10.13	0.42	2.48	724.55	354.32	1078.64	147.05
XSs	2.08	0.41	3.52	138.64	469.09	607.73	207.05
GDs	16.48	0.71	7.60	912.73	841.82	1754.55	381.36
SKs	4.00	0.72	1.74	114.77	100.23	215.00	29.55
YDs	14.11	1.75	13.10	386.82	718.64	1105.45	311.14
FLXs	40.38	7.74	4.46	589.77	130.45	720.23	-47.73
SJs	41.36	9.27	11.05	536.59	286.82	823.41	23.18

501

502 **6 Conclusions**

503 This study revealed the temporary and net sinks of atmospheric CO_2 due to chemical
504 weathering in a subtropical hyperactive catchment with mixing carbonate and silicate lithology
505 under the stress of chemical weathering induced by anthropogenic sulfuric acid agent. During the
506 sampling period, the pH values ranged from 7.5 to 8.5 and TDS varied from 73.8 to 230.2 mg·L^{-1}.
507 Ca^{2+} and HCO_3^- were the dominated cation and anion. Water chemical patterns and PCA showed
508 that carbonate and silicate weathering were the most important processes controlling the local
509 hydrochemistry. In average, carbonate and silicate weathering contributed approximately 50.06%

https://doi.org/10.5194/bg-2019-310
Preprint. Discussion started: 13 November 2019

and 25.71% of the total cationic loads, respectively.

The average of carbonate and silicate weathering rate in the Beijiang River Basin were 61.15 and 25.31 $t \cdot km^{-2} \cdot a^{-1}$, respectively. The high rate was comparable to other rivers located in the hyperactive zone between the latitude 0-30°. The lithology, runoff and geomorphology had significant influence on the chemical weathering rate. (1) Due to the difference between kinetics of carbonate and silicate dissolution processes, the proportion of carbonate outcrops had significant positive correlation with the chemical weathering rate and confirmed that carbonate outcrops ratios was the sensitive factor controlling the chemical weathering rates and the rapid kinetics of carbonate dissolution played an important role in weathering rates. (2) Runoff manly controlled the season variations and the dilution effect was weak in the study area. Due to the compensation effect of chemical weathering, significant positive linear relationship was detected between Q and TWR, CWR and SWR. (3) The geomorphology factors such as slope and HI had non-linear correlation on chemical weathering rate and showed significant scale effect, which revealed the complexity in chemical weathering processes.

DIC apportionment showed that CCW was the dominant origin of DIC (35%-87%) and that SCW (3%-15%) and CSW (7%-59%) were non-negligible weathering processes. The CCR_{Total} was 823.41 10^3 mol km^{-2} a^{-1}, relative high CCR due to high chemical weathering rate. In addition, the CCR_{CCW} and CCR_{CSW} were 536.59×10^3 (65%) and 286.82×10^3 (35%) mol km^{-2} a^{-1}, respectively. Compared with the "temporary" sink, the net sink of CO_2 for the Beijiang River was approximately 23.18×10^3 mol km^{-2} a^{-1} of CO_2 sinking in the perspective of global carbon cycling. It was about 2.82% of the "temporary" CO_2 sink. Human activities induced sulfur acid deposition and AMD have significantly alter the CO_2 sinks.

https://doi.org/10.5194/bg-2019-310
Preprint. Discussion started: 13 November 2019

7 Acknowledgments

This research work was financially supported by the General Program of the National Natural Science Foundation of China (No.41877470), the Natural Science Foundation of Guangdong Province, China (No. 2017A030313231) and the Natural Science Foundation of Guangdong Province, China (No. 2017A030313229).

8 Code/Data availability: Yes.

9 Author contribution: Cao Yingjie and Tang Changyuan designed the study, carried out the field work, analyzed the results, and drafted the manuscript. Xuan Yingxue and Guan Shuai participated in the field sampling and laboratory analysis. Peng Yisheng reviewed and edited the original draft of the manuscript. All authors read and approved the final manuscript.

10 Competing interests: No.

References

Appelo, C. A. J., and Postma, D.: Geochemistry, groundwater and pollution, CRC press, 2005.

Berner, R. A., and Kothavala, Z.: GEOCARB III: a revised model of atmospheric CO_2 over Phanerozoic time, American Journal of Science, 301, 182-204, 0002-9599, 2001.

Cao, Y., Tang, C., Song, X., and Liu, C.: Major ion chemistry, chemical weathering and CO_2 consumption in the Songhua River basin, Northeast China, Environmental Earth Sciences, 73, 7505-7516, 10.1007/s12665-014-3921-2, 2015.

Cao, Y., Tang, C., Cao, G., and Wang, X.: Hydrochemical zoning: natural and anthropogenic origins of the major elements in the surface water of Taizi River Basin, Northeast China, Environmental Earth Sciences, 75, 811, 10.1007/s12665-016-5469-9, 2016a.

Cao, Y., Tang, C., Cao, G., and Wang, X.: Hydrochemical zoning: natural and anthropogenic origins of the major elements in the surface water of Taizi River Basin, Northeast China, Environmental Earth Sciences, 75, 1-14, 2016b.

Chen, J., Wang, F., Xia, X., and Zhang, L.: Major element chemistry of the Changjiang (Yangtze River), Chemical Geology, 187, 231-255, 2002a.

Chen, J., Wang, F., Xia, X., and Zhang, L.: Major element chemistry of the Changjiang (Yangtze River), Chemical Geology, 187, 231-255, 2002b.

Chen, J., Wang, F., Meybeck, M., He, D., Xia, X., and Zhang, L.: Spatial and temporal analysis of water chemistry records (1958–2000) in the Huanghe (Yellow River) basin, Global biogeochemical cycles, 19, 2005.

Ding, H., Liu, C.-Q., Zhao, Z.-Q., Li, S.-L., Lang, Y.-C., Li, X.-D., Hu, J., and Liu, B.-J.: Geochemistry of the dissolved loads of the Liao River basin in northeast China under anthropogenic pressure: Chemical weathering and controlling factors, Journal of Asian Earth

https://doi.org/10.5194/bg-2019-310
Preprint. Discussion started: 13 November 2019

566 Sciences, 138, 657-671, https://doi.org/10.1016/j.jseaes.2016.07.026, 2017.
567 Donnini, M., Frondini, F., Probst, J.-L., Probst, A., Cardellini, C., Marchesini, I., and Guzzetti, F.:
568 Chemical weathering and consumption of atmospheric carbon dioxide in the Alpine region,
569 Global and Planetary Change, 136, 65-81, https://doi.org/10.1016/j.gloplacha.2015.10.017,
570 2016.
571 Dosseto, A., Bourdon, B., Gaillardet, J., Allègre, C. J., and Filizola, N.: Time scale and conditions
572 of weathering under tropical climate: Study of the Amazon basin with U-series, Geochimica et
573 Cosmochimica Acta, 70, 71-89, https://doi.org/10.1016/j.gca.2005.06.033, 2006.
574 Edmond, J. M., Palmer, M. R., Measures, C. I., Brown, E. T., and Huh, Y.: Fluvial geochemistry of
575 the eastern slope of the northeastern Andes and its foredeep in the drainage of the Orinoco in
576 Colombia and Venezuela, Geochimica et Cosmochimica Acta, 60, 2949-2974,
577 https://doi.org/10.1016/0016-7037(96)00142-1, 1996.
578 Eiriksdottir, E. S., Gislason, S. R., and Oelkers, E. H.: Does runoff or temperature control chemical
579 weathering rates?, Applied Geochemistry, 26, S346-S349,
580 https://doi.org/10.1016/j.apgeochem.2011.03.056, 2011.
581 Fernandes, A. M., Conceição, F. T. d., Spatti Junior, E. P., Sardinha, D. d. S., and Mortatti, J.:
582 Chemical weathering rates and atmospheric/soil CO_2 consumption of igneous and
583 metamorphic rocks under tropical climate in southeastern Brazil, Chemical Geology, 443, 54-
584 66, https://doi.org/10.1016/j.chemgeo.2016.09.008, 2016.
585 Gaillardet, J., Dupré, B., Louvat, P., and Allègre, C. J.: Global silicate weathering and CO2
586 consumption rates deduced from the chemistry of large rivers, Chemical Geology, 159, 3-30,
587 https://doi.org/10.1016/S0009-2541(99)00031-5, 1999a.
588 Gaillardet, J., Dupré, B., Louvat, P., and Allègre, C. J.: Global silicate weathering and CO2
589 consumption rates deduced from the chemistry of large rivers, Chemical Geology, 159, 3-30,
590 https://doi.org/10.1016/S0009-2541(99)00031-5, 1999b.
591 Galy, A., and France-Lanord, C.: Weathering processes in the Ganges–Brahmaputra basin and the
592 riverine alkalinity budget, Chemical Geology, 159, 31-60, https://doi.org/10.1016/S0009-
593 2541(99)00033-9, 1999.
594 Gao, Q., Tao, Z., Huang, X., Nan, L., Yu, K., and Wang, Z.: Chemical weathering and CO2
595 consumption in the Xijiang River basin, South China, Geomorphology, 106, 324-332,
596 https://doi.org/10.1016/j.geomorph.2008.11.010, 2009.
597 Garrels, R. M.: The carbonate-silicate geochemical cycle and its effect on atmospheric carbon
598 dioxide over the past 100 million years, Am J Sci, 283, 641-683, 1983.
599 Gibbs, R. J.: Water chemistry of the Amazon River, Geochimica et Cosmochimica Acta, 36, 1061-
600 1066, https://doi.org/10.1016/0016-7037(72)90021-X, 1972.
601 Gislason, S. R., Oelkers, E. H., Eiriksdottir, E. S., Kardjilov, M. I., Gisladottir, G., Sigfusson, B.,
602 Snorrason, A., Elefsen, S., Hardardottir, J., Torssander, P., and Oskarsson, N.: Direct evidence
603 of the feedback between climate and weathering, Earth and Planetary Science Letters, 277,
604 213-222, https://doi.org/10.1016/j.epsl.2008.10.018, 2009.
605 Guo, J., Wang, F., Vogt, R. D., Zhang, Y., and Liu, C. Q.: Anthropogenically enhanced chemical
606 weathering and carbon evasion in the Yangtze Basin, Scientific Reports, 5, 11941, 2015.
607 Hagedorn, B., and Cartwright, I.: Climatic and lithologic controls on the temporal and spatial
608 variability of CO_2 consumption via chemical weathering: An example from the Australian
609 Victorian Alps, Chemical Geology, 260, 234-253,

https://doi.org/10.5194/bg-2019-310
Preprint. Discussion started: 13 November 2019

610 https://doi.org/10.1016/j.chemgeo.2008.12.019, 2009.
611 Hartmann, J., Jansen, N., Dürr, H. H., Kempe, S., and Köhler, P.: Global CO_2-consumption by
612 chemical weathering: What is the contribution of highly active weathering regions?, Global
613 and Planetary Change, 69, 185-194, https://doi.org/10.1016/j.gloplacha.2009.07.007, 2009.
614 Hartmann, J., Moosdorf, N., Lauerwald, R., Hinderer, M., and West, A. J.: Global chemical
615 weathering and associated P-release - The role of lithology, temperature and soil properties,
616 Chemical Geology, 363, 145-163, https://doi.org/10.1016/j.chemgeo.2013.10.025, 2014a.
617 Hartmann, J., West, J., Renforth, P., Köhler, P., Rocha, C. D. L., Wolf-Gladrow, D., Dürr, H., and
618 Scheffran, J.: Enhanced chemical weathering as a sink for carbon dioxide, a nutrient source
619 and a strategy to mitigate ocean acidification, Reviews of Geophysics, 2014b.
620 He Jiangyi, Z. D., Zhao zhiqi: Spatial and temporal variations in hydrochemical composition of
621 river water in Yellow River Basin, China, Chinese Journal of Ecology, 1-12, 2017.
622 Hercod, D. J., Brady, P. V., and Gregory, R. T.: Catchment-scale coupling between pyrite oxidation
623 and calcite weathering, Chemical Geology, 151, 259-276, https://doi.org/10.1016/S0009-
624 2541(98)00084-9, 1998.
625 Huh, Y., and Edmond, J. M.: The fluvial geochemistry of the rivers of Eastern Siberia: III.
626 Tributaries of the Lena and Anabar draining the basement terrain of the Siberian Craton and
627 the Trans-Baikal Highlands, Geochimica et Cosmochimica Acta, 63, 967-987,
628 https://doi.org/10.1016/S0016-7037(99)00045-9, 1999.
629 Jiang, H., Liu, W., Xu, Z., Zhou, X., Zheng, Z., Zhao, T., Zhou, L., Zhang, X., Xu, Y., and Liu, T.:
630 Chemical weathering of small catchments on the Southeastern Tibetan Plateau I: Water sources,
631 solute sources and weathering rates, Chemical Geology, 500, 159-174,
632 https://doi.org/10.1016/j.chemgeo.2018.09.030, 2018.
633 Kempe, S., and Degens, E. T.: An early soda ocean?, Chemical Geology, 53, 95-108,
634 https://doi.org/10.1016/0009-2541(85)90023-3, 1985.
635 Khadka, M. B., Martin, J. B., and Jin, J.: Transport of dissolved carbon and CO_2 degassing from a
636 river system in a mixed silicate and carbonate catchment, Journal of Hydrology, 513, 391-402,
637 https://doi.org/10.1016/j.jhydrol.2014.03.070, 2014.
638 Larssen, T., and Carmichael, G. R.: Acid rain and acidification in China: the importance of base
639 cation deposition, Environmental Pollution, 110, 89-102, https://doi.org/10.1016/S0269-
640 7491(99)00279-1, 2000.
641 Larssen, T., Lydersen, E., Tang, D., He, Y., Gao, J., Liu, H., Duan, L., Seip, H. M., Vogt, R. D.,
642 Mulder, J., Shao, M., Wang, Y., Shang, H., Zhang, X., Solberg, S., Aas, W., Okland, T.,
643 Eilertsen, O., Angell, V., Li, Q., Zhao, D., Xiang, R., Xiao, J., and Luo, J.: Acid Rain in China,
644 Environmental Science & Technology, 40, 418-425, 10.1021/es0626133, 2006.
645 Lenton, T. M., and Britton, C.: Enhanced carbonate and silicate weathering accelerates recovery
646 from fossil fuel CO2 perturbations, Global Biogeochemical Cycles, 20,
647 10.1029/2005gb002678, 2006.
648 Li, R., Tang, C., Cao, Y., Jiang, T., and Chen, J.: The distribution and partitioning of trace metals
649 (Pb, Cd, Cu, and Zn) and metalloid (As) in the Beijiang River, Environmental Monitoring and
650 Assessment, 190, 399, 10.1007/s10661-018-6789-x, 2018.
651 Li, R., Tang, C., Li, X., Jiang, T., Shi, Y., and Cao, Y.: Reconstructing the historical pollution levels
652 and ecological risks over the past sixty years in sediments of the Beijiang River, South China,
653 Science of The Total Environment, 649, 448-460,

https://doi.org/10.5194/bg-2019-310
Preprint. Discussion started: 13 November 2019

654 https://doi.org/10.1016/j.scitotenv.2018.08.283, 2019.
655 Li, S.-L., Calmels, D., Han, G., Gaillardet, J., and Liu, C.-Q.: Sulfuric acid as an agent of carbonate
656 weathering constrained by $\delta^{13}C_{DIC}$: Examples from Southwest China, Earth and Planetary
657 Science Letters, 270, 189-199, https://doi.org/10.1016/j.epsl.2008.02.039, 2008.
658 Li, S., Lu, X. X., He, M., Zhou, Y., Bei, R., Li, L., and Ziegler, A. D.: Major element chemistry in
659 the upper Yangtze River: A case study of the Longchuanjiang River, Geomorphology, 129, 29-
660 42, https://doi.org/10.1016/j.geomorph.2011.01.010, 2011.
661 Li, S., Lu, X. X., and Bush, R. T.: Chemical weathering and CO_2 consumption in the Lower Mekong
662 River, Science of The Total Environment, 472, 162-177,
663 https://doi.org/10.1016/j.scitotenv.2013.11.027, 2014.
664 Liu, B., Liu, C.-Q., Zhang, G., Zhao, Z.-Q., Li, S.-L., Hu, J., Ding, H., Lang, Y.-C., and Li, X.-D.:
665 Chemical weathering under mid- to cool temperate and monsoon-controlled climate: A study
666 on water geochemistry of the Songhuajiang River system, northeast China, Applied
667 Geochemistry, 31, 265-278, https://doi.org/10.1016/j.apgeochem.2013.01.015, 2013.
668 Liu, Z., Dreybrodt, W., and Liu, H.: Atmospheric CO_2 sink: Silicate weathering or carbonate
669 weathering?, Applied Geochemistry, 26, S292-S294,
670 https://doi.org/10.1016/j.apgeochem.2011.03.085, 2011.
671 Liu, Z., and Dreybrodt, W.: Significance of the carbon sink produced by H_2O–carbonate–CO_2–
672 aquatic phototroph interaction on land, Science Bulletin, 60, 182-191, 2095-9273, 2015.
673 Ludwig, W., Amiotte-Suchet, P., Munhoven, G., and Probst, J.-L.: Atmospheric CO2 consumption
674 by continental erosion: present-day controls and implications for the last glacial maximum,
675 Global and Planetary Change, 16-17, 107-120, https://doi.org/10.1016/S0921-8181(98)00016-
676 2, 1998.
677 Meybeck, M., Dürr, H. H., and Vörösmarty, C. J.: Global coastal segmentation and its river
678 catchment contributors: A new look at land-ocean linkage, Global Biogeochemical Cycles, 20,
679 10.1029/2005gb002540, 2006.
680 Mora, A., Baquero, J. C., Alfonso, J. A., Pisapia, D., and Balza, L.: The Apure River: geochemistry
681 of major and selected trace elements in an Orinoco River tributary coming from the Andes,
682 Venezuela, Hydrological Processes, 24, 3798-3810, 10.1002/hyp.7801, 2010.
683 Mortatti, J., and Probst, J.-L.: Silicate rock weathering and atmospheric/soil CO2 uptake in the
684 Amazon basin estimated from river water geochemistry: seasonal and spatial variations,
685 Chemical Geology, 197, 177-196, https://doi.org/10.1016/S0009-2541(02)00349-2, 2003.
686 Négrel, P., Allègre, C. J., Dupré, B., and Lewin, E.: Erosion sources determined by inversion of
687 major and trace element ratios and strontium isotopic ratios in river water: The Congo Basin
688 case, Earth and Planetary Science Letters, 120, 59-76, https://doi.org/10.1016/0012-
689 821X(93)90023-3, 1993.
690 Ollivier, P., Hamelin, B., and Radakovitch, O.: Seasonal variations of physical and chemical erosion:
691 A three-year survey of the Rhone River (France), Geochimica et Cosmochimica Acta, 74, 907-
692 927, https://doi.org/10.1016/j.gca.2009.10.037, 2010.
693 PIKE, R. J., and WILSON, S. E.: Elevation-Relief Ratio, Hypsometric Integral, and Geomorphic
694 Area-Altitude Analysis, GSA Bulletin, 82, 1079-1084, 10.1130/0016-
695 7606(1971)82[1079:erhiag]2.0.co;2, 1971.
696 Ran, X., Yu, Z., Yao, Q., Chen, H., and Mi, T.: Major ion geochemistry and nutrient behaviour in
697 the mixing zone of the Changjiang (Yangtze) River and its tributaries in the Three Gorges

https://doi.org/10.5194/bg-2019-310
Preprint. Discussion started: 13 November 2019

698 Reservoir, Hydrological processes, 24, 2481-2495, 2010.
699 Rao, W., Zheng, F., Tan, H., Yong, B., Jin, K., Wang, S., Zhang, W., Chen, T., and Wang, Y.: Major
700 ion chemistry of a representative river in South-central China: Runoff effects and controlling
701 mechanisms, Journal of Hazardous Materials, 378, 120755,
702 https://doi.org/10.1016/j.jhazmat.2019.120755, 2019.
703 Ryu, J.-S., Lee, K.-S., Chang, H.-W., and Shin, H. S.: Chemical weathering of carbonates and
704 silicates in the Han River basin, South Korea, Chemical Geology, 247, 66-80,
705 https://doi.org/10.1016/j.chemgeo.2007.09.011, 2008.
706 Singh, O., Sarangi, A., and Sharma, M. C.: Hypsometric Integral Estimation Methods and its
707 Relevance on Erosion Status of North-Western Lesser Himalayan Watersheds, Water
708 Resources Management, 22, 1545-1560, 10.1007/s11269-008-9242-z, 2008.
709 Spence, J., and Telmer, K.: The role of sulfur in chemical weathering and atmospheric CO_2 fluxes:
710 Evidence from major ions, $\delta^{13}C_{DIC}$, and $\delta^{34}S_{SO4}$ in rivers of the Canadian Cordillera,
711 Geochimica et Cosmochimica Acta, 69, 5441-5458, https://doi.org/10.1016/j.gca.2005.07.011,
712 2005.
713 Stallard, R. F., and Edmond, J. M.: Geochemistry of the Amazon: 1. Precipitation chemistry and the
714 marine contribution to the dissolved load at the time of peak discharge, Journal of Geophysical
715 Research: Oceans, 86, 9844-9858, 10.1029/JC086iC10p09844, 1981.
716 Stallard, R. F., and Edmond, J. M.: Geochemistry of the Amazon: 2. The influence of geology and
717 weathering environment on the dissolved load, Journal of Geophysical Research: Oceans, 88,
718 9671-9688, 10.1029/JC088iC14p09671, 1983.
719 Stallard, R. F., and Edmond, J. M.: Geochemistry of the Amazon: 3. Weathering chemistry and limits
720 to dissolved inputs, Journal of Geophysical Research: Oceans, 92, 8293-8302,
721 10.1029/JC092iC08p08293, 1987.
722 STRAHLER, A. N.: HYPSOMETRIC (AREA-ALTITUDE) ANALYSIS OF EROSIONAL
723 TOPOGRAPHY, GSA Bulletin, 63, 1117-1142, 10.1130/0016-
724 7606(1952)63[1117:haaoet]2.0.co;2, 1952.
725 Sun, X., Mörth, C.-M., Humborg, C., and Gustafsson, B.: Temporal and spatial variations of rock
726 weathering and CO2 consumption in the Baltic Sea catchment, Chemical Geology, 466, 57-69,
727 https://doi.org/10.1016/j.chemgeo.2017.04.028, 2017.
728 Taylor, B. E., Wheeler, M. C., and Nordstrom, D. K.: Stable isotope geochemistry of acid mine
729 drainage: Experimental oxidation of pyrite, Geochimica et Cosmochimica Acta, 48, 2669-2678,
730 https://doi.org/10.1016/0016-7037(84)90315-6, 1984.
731 van Everdingen, R. O., and Krouse, H. R.: Isotope composition of sulphates generated by bacterial
732 and abiological oxidation, Nature, 315, 395-396, 10.1038/315395a0, 1985.
733 Viers, J., Oliva, P., Dandurand, J. L., Dupré, B., and Gaillardet, J.: Chemical weathering rates, CO2
734 consumption, and control parameters deduced from the chemical composition of rivers, 2014.
735 Walling, D. E.: Solute in river systems, Solute Processes, 251-327, 1986.
736 Wen, J., Tang, C., Cao, Y., Li, X., and Chen, Q.: Hydrochemical evolution of groundwater in a
737 riparian zone affected by acid mine drainage (AMD), South China: the role of river–
738 groundwater interactions and groundwater residence time, Environmental Earth Sciences, 77,
739 794, 10.1007/s12665-018-7977-2, 2018.
740 Wu, W., Xu, S., Yang, J., and Yin, H.: Silicate weathering and CO_2 consumption deduced from the
741 seven Chinese rivers originating in the Qinghai-Tibet Plateau, Chemical Geology, 249, 307-

https://doi.org/10.5194/bg-2019-310
Preprint. Discussion started: 13 November 2019

320, 2008.

Xie chenji, G. Q., Tao zhen, Liu Longhai, Lishanchi: Chemical weathering and CO_2 consumption in the Dongjiang River Basin, Acta Scientiae Circumstantiae, 33, 2123-2133, 2013.

Xiong, L., Tang, G., Yuan, B., Lu, Z., Li, F., and Zhang, L.: Geomorphological inheritance for loess landform evolution in a severe soil erosion region of Loess Plateau of China based on digital elevation models, Science China Earth Sciences, 57, 1944-1952, 10.1007/s11430-014-4833-4, 2014.

Xu, Z., and Liu, C.-Q.: Water geochemistry of the Xijiang basin rivers, South China: Chemical weathering and CO_2 consumption, Applied Geochemistry, 25, 1603-1614, 2010.

Zeng, C., Liu, Z., Zhao, M., and Yang, R.: Hydrologically-driven variations in the karst-related carbon sink fluxes: Insights from high-resolution monitoring of three karst catchments in Southwest China, Journal of Hydrology, 533, 74-90, https://doi.org/10.1016/j.jhydrol.2015.11.049, 2016.

Zhang, J., Huang, W., Letolle, R., and Jusserand, C.: Major element chemistry of the Huanghe (Yellow River), China-weathering processes and chemical fluxes, Journal of Hydrology, 168, 173-203, 1995.

Zhang, L., Song, X., Xia, J., Yuan, R., Zhang, Y., Liu, X., and Han, D.: Major element chemistry of the Huai River basin, China, Applied Geochemistry, 26, 293-300, 2011.

Zhang, S. R., Lu, X. X., Higgitt, D. L., Chen, C. T. A., Sun, H. G., and Han, J. T.: Water chemistry of the Zhujiang (Pearl River): natural processes and anthropogenic influences. Journal of Geophysical Research, 112(F1), F01011, Journal of Geophysical Research Atmospheres, 112, 137-161, 2007a.

Zhang, S. R., Lu, X. X., Higgitt, D. L., Chen, C. T. A., Sun, H. G., and Han, J. T.: Water chemistry of the Zhujiang (Pearl River): Natural processes and anthropogenic influences, Journal of Geophysical Research: Earth Surface (2003–2012), 112, 10.1029/2006JF000493, 2007b.